INORGANIC CHEMISTRY FRONTIERS

RESEARCH ARTICLE

View Article Online
View Journal | View Issue

Cite this: *Inorg. Chem. Front.*, 2025, **12**, 5054

Harnessing the dual role of DMSO in the synthesis of SbOCl·DMSO: an excellent nonlinear optical crystal with unique 1D spiral chain†

Xiande Peng,[a] Xiangyuan Li,[a] Yingzi Zhang,[a] Xuehua Dong,*[a] Ling Huang,[a] Liling Cao,[a] Daojiang Gao[a] and Guohong Zou*[b]

Received 15th March 2025,
Accepted 22nd April 2025

DOI: 10.1039/d5qi00758e

rsc.li/frontiers-inorganic

Nonlinear optical (NLO) materials are essential for applications such as laser micromachining and optical parametric oscillations. An ideal NLO material should exhibit a large second-harmonic generation (SHG) coefficient, moderate birefringence and a short cut-off edge. However, achieving these properties simultaneously in a single material remains a significant challenge due to their distinct structural requirements. In this study, we report the synthesis of a novel NLO material, $SbOCl{\cdot}SO(CH_3)_2$ (SbOCl·DMSO), which features an optimized 1D helical chain structure. For the first time, the polar organic molecule dimethyl sulfoxide (DMSO) is introduced into the $SbCl_3$ system, where it coordinates with an Sb atom *via* Sb–O bonds, modifying the chain structure. This unique 1D $[SbOCl]_\infty$ helical chain enhances the compound's polarizability and optical anisotropy, leading to excellent optical properties. SbOCl·DMSO exhibits a large SHG coefficient of 4.4 × KDP at 1064 nm, moderate birefringence of 0.084@546 nm and a short UV cut-off edge of 331 nm, making it a highly promising candidate for NLO applications. This work highlights the importance of synergistic molecular design and provides a new strategy for the development of high-performance frequency-doubling crystals.

Introduction

Nonlinear optical (NLO) materials are essential components in ultraviolet (UV) solid-state lasers, which have widespread applications in laser-driven technologies such as laser photolithography, quantum entanglement, medical treatments, and laser micromachining.[1–12] Efficient screening of NLO crystals with high conversion efficiency under intense laser irradiation remains a significant challenge. To be effective in UV NLO applications, an ideal crystal must exhibit the following key properties: a large NLO coefficient ($d_{ij} \geq 0.39$ pm V^{-1}), moderate birefringence (0.06–0.12) and a short UV cut-off wavelength (≤400 nm).[13–16] However, achieving these properties simultaneously is particularly difficult due to the conflicting structural requirements for the second-harmonic generation (SHG) effect and bandgap optimization.[17,18] Therefore, it is imperative to explore innovative strategies that can balance these optical properties and meet all three criteria.

In light of the correlation between structural characteristics and optical properties, the microscopic properties of functional groups determine the macroscopic properties of compounds.[19,20] Functional groups with high polarizability and optical anisotropy are beneficial for compounds to exhibit high frequency doubling effect and large birefringence. Recently, multiple researchers have proposed that the incorporation of metal cation twisted polyhedral, particularly those featuring stereochemically active lone pair (SCALP) electrons, will substantially promote total optical anisotropy and polarizability based on theoretical calculations,[21,22] such as Sn_2PO_4I (0.664@546 nm),[23] $(C_5H_5NO)(Sb_2OF_4)$ (12 × KDP, 0.513@546 nm),[24] $(SbTeO_3)(NO_3)$ (2.2 × KDP, 0.081@546 nm),[25] *etc.* Interestingly, the metals (M) with SCALP electronics exhibit rich coordination modes, *e.g.* $[MO_5]$ square pyramid, $[MO_4]$ seesaw and $[MO_3]$ triangular pyramid, which is beneficial for the target compound to exhibit a rich structure. However, it is worth noting that these systems containing SCALP electrons are prone to oxidation in air and hydrolysis in water, and there is an urgent need to explore appropriate strategies to address this issue.[26–29] Recently, our research group has successfully synthesized a series of high-

[a]*College of Chemistry and Materials Science, Sichuan Normal University, Chengdu, 610066, P. R. China. E-mail: dongxh027@sina.com*
[b]*College of Chemistry, Sichuan University, Chengdu, 610065, P. R. China. E-mail: zough@scu.edu.cn*

†Electronic supplementary information (ESI) available: Additional crystallographic data, the bond lengths information, the crystal stability test, TGA, PXRD for the residue of TGA, IR spectrum, band structure. CCDC 2371835 for SbOCl·DMSO. For ESI and crystallographic data in CIF or other electronic format see DOI: https://doi.org/10.1039/d5qi00758e

performance frequency doubling crystals by introducing solvent-free synthesis, ionothermal synthesis, and low-temperature molten salt synthesis, methanol evaporation synthesis and other methods, such as $GeHPO_3$ (10.3 × KDP, 0.062@546 nm),[30] $Rb_2SbFP_2O_7$ (5.1 × KDP, 0.15@546 nm),[31] $CsSbF_2SO_4$ (3 × KDP, 0.112@546 nm),[32] $RbSbSO_4Cl_2$ (2.7 × KDP, 0.11@546 nm).[33]

In our continued exploration of synthesis methods, we found that polar organic molecule dimethyl sulfoxide (DMSO) serves multiple roles. First, it acts as a versatile solvent, capable of dissolving both polar and non-polar compounds, including various inorganic salts, organic molecules, and polymers. Its exceptional solubility promotes the efficient dissolution and uniform distribution of reactants, thus accelerating chemical reactions. Second, the near-neutral environment provided by DMSO effectively prevents the hydrolysis of metal cations (*e.g.*, Sb^{3+}, Ge^{2+}, Sn^{2+}), making it particularly suitable for reactions sensitive to hydrolysis. Third, the oxygen atom in DMSO, which possesses a lone pair of electrons, can form coordination bonds with metal ions[34]—an attribute frequently leveraged in the design and synthesis of metal complexes (Fig. 1). Upon coordination, DMSO induces structural distortions that enhance the anisotropy and polarizability of the resulting compound, subsequently improving its optical properties. These characteristics make DMSO especially valuable in the development of NLO materials.

However, the introduction of metal polyhedra containing SCALP into the system often results in a red shift in the compound's band gap, making further enhancement of the band gap increasingly difficult. This limitation poses a significant challenge for their practical applications in the UV region.[35,36] Previous studies have often addressed this issue by introducing highly electronegative, relatively light halogen elements (such as F and Cl) to reduce orbital overlap, thereby widening the band gap, improving UV transparency, and optimizing the UV cut-off edge. Examples include compounds such as $NH_4B_4O_6F$[37] and $ABiCl_2SO_4$ (A = NH_4, K, Rb).[38] Furthermore, halide ions, due to their relatively large anionic polarizability, can substantially enhance the overall polarizability of crystals, thereby improving their nonlinear optical properties. Consequently, by carefully selecting and incorporating halogens, it is possible to effectively tune critical properties of compounds, including the band gap, polarizability and birefringence.

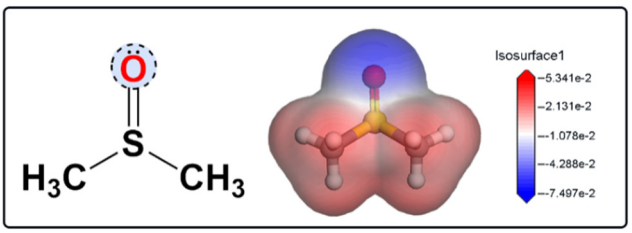

Fig. 1 Active bidentate sites locate on [DMSO]. Electrostatic potential map on [DMSO].

Guided by the insights from previous research, we explored a system containing SCALP electrons using DMSO as both a reactant and solvent, while incorporating halide ions into the system. This approach led to the successful development of an exceptional UV NLO crystal, $SbOCl{\cdot}SO(CH_3)_2$ (SbOCl·DMSO). Notably, in this compound, the DMSO molecule is coordinated to the $[SbOCl]_\infty$ 1D chain through an Sb–O bond, marking a novel feature in existing Sb-based systems. It is well-established that in one-dimensional (1D) structures, the orderly arrangement of chain units along a specific direction facilitates more regular charge distribution, which enhances polarizability and anisotropy. This, in turn, improves the compound's nonlinear optical effects and birefringence. The optimized 1D chain structure enables perfect synergy between the [DMSO] and $[SbO_3Cl]^{4-}$ bifunctional groups, resulting in an excellent balance of optical properties, including a large second-harmonic generation (SHG) coefficient (4.4 × KDP), moderate birefringence (0.084@546 nm) and a short UV cut-off edge (331 nm). These properties suggest that SbOCl·DMSO is a highly promising NLO material. This study offers valuable structural design insights for the future synthesis of high-performance NLO crystals containing SCALP electrons.

Results and discussion

Crystal synthesis

$SbCl_3$ (99.9%, Aaladdin) and DMSO (78.1%, Keshi) were obtained from commercial sources in analytical grade and used without additional purification.

SbOCl·DMSO crystals were successfully synthesized using the solvent evaporation method (Fig. 2a). Initially, $SbCl_3$ (0.228 g, 1 mmol) and DMSO (2 mL) were mixed in a beaker, and stirred until it is completely dissolved. The solvent was then allowed to evaporate at room temperature over a period of 5 days. During this process, Sb atoms effectively coordinated with oxygen atoms from DMSO, forming Sb–O coordination bonds, which led to the precipitation of block-shaped, transparent SbOCl·DMSO crystals. The yield of the crystals was 46% (based on Sb) (insert of Fig. 3b).

Crystal structures

The SbOCl·DMSO compound, composed of two independent Sb atoms, two Cl atoms, four O atoms, and two independent DMSO molecules (Fig. 2b), crystallizes in the orthorhombic space group $Pca2_1$ (no. 29). In this structure, each Sb atom is three-coordinated to two O atoms and one Cl atom, forming a $[SbO_2Cl]^{2-}$ trigonal pyramid (Fig. 2c). The DMSO molecules are integrated into this chain through Sb–O coordination bonds, with bond lengths ranging from 2.225 to 2.246 Å, resulting in a $[SbOCl{\cdot}DMSO]_\infty$ 1D organic–inorganic hybrid spiral chain. The Sb atom ultimately adopts the $[SbO_3Cl]^{4-}$ coordination mode (Fig. 2d). This hybrid chain significantly enhances the compound's polarizability and optical anisotropy (Fig. 2e). Finally, these chains are assembled into a 3D framework *via* van der Waals interactions (Fig. 2f).

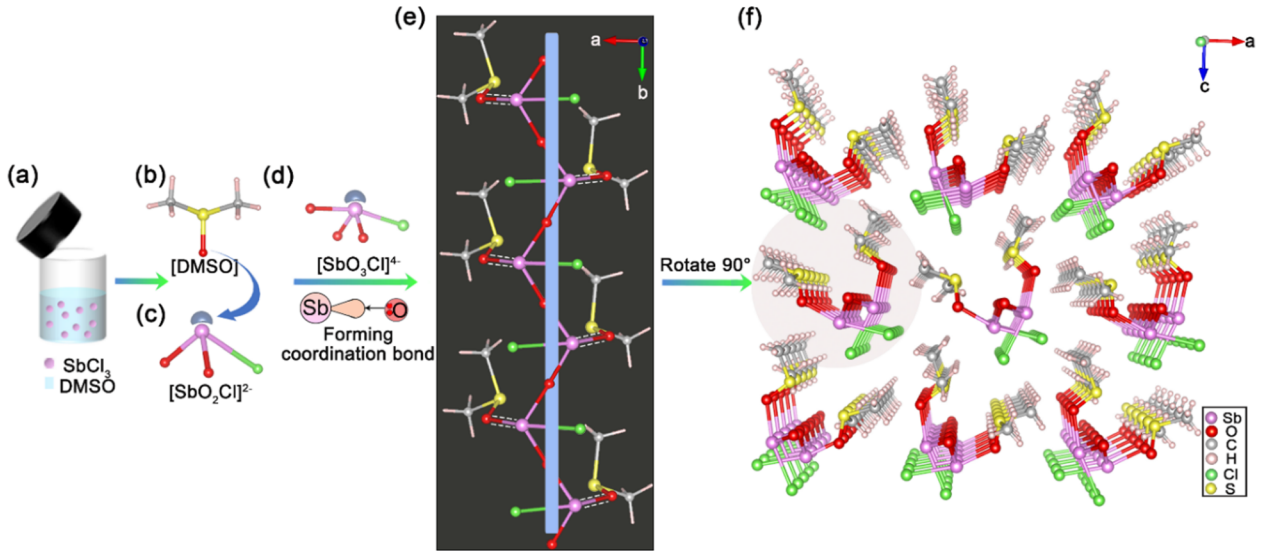

Fig. 2 (a) Schematic diagram of the synthetic route; ball and stick representations of (b) the [DMSO] and (c) $[SbO_2Cl]^{2-}$ triangular pyramids; (d) $[SbO_3Cl]^{4-}$ seesaw; (e) the 1D $[SbOClDMSO]_\infty$ organic–inorganic hybrid spiral chain; (f) the 3D framework structure of SbOCl·DMSO viewed in the *ac* plane.

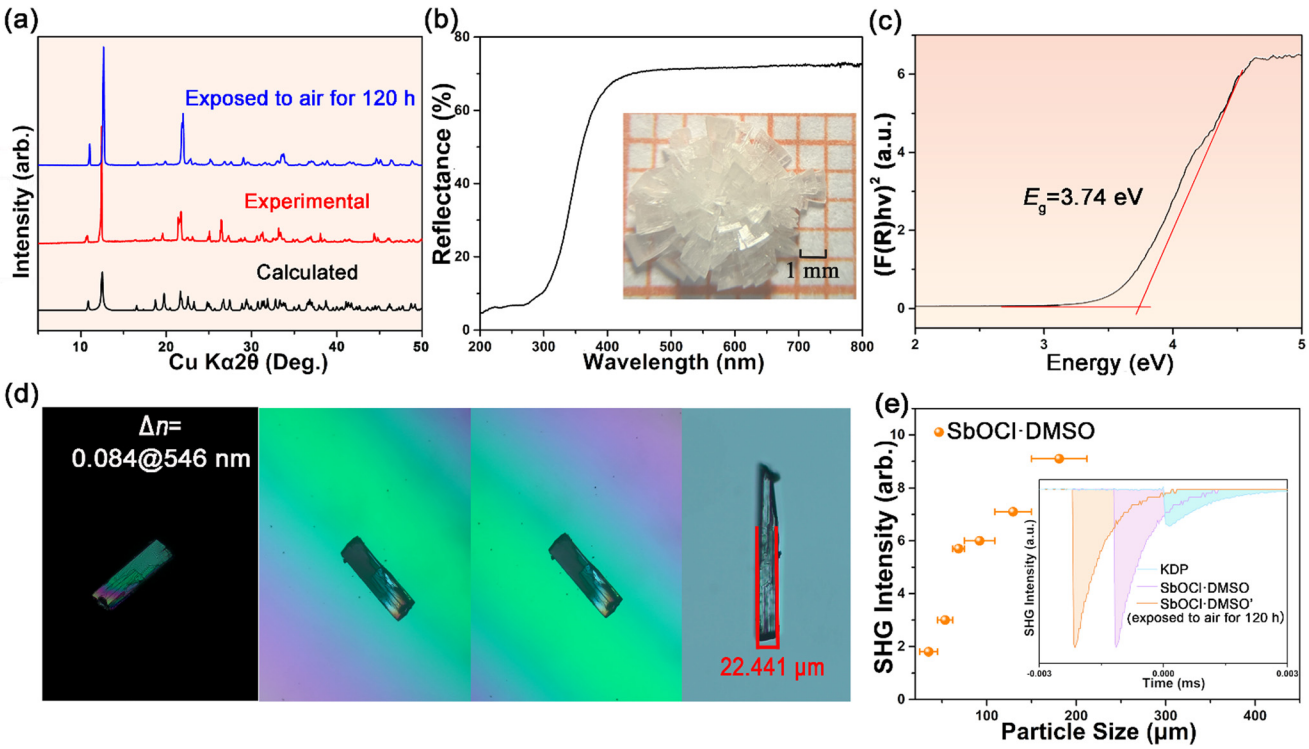

Fig. 3 (a) XRD patterns of the SbOCl·DMSO; (b and c) UV-vis diffuse reflectance spectra for SbOCl·DMSO (the insert of (b) is the image of SbOCl·DMSO crystals); (d) birefringence measurement on the SbOCl·DMSO crystal; (e) phase-matching curve of SbOCl·DMSO (the insert is the SHG signals of SbOCl·DMSO and SbOCl·DMSO′-after being exposed under humid air at room temperature for more than 120 h).

Chemical phase and stability analysis

As shown in Fig. 3a, the powder X-ray diffraction (PXRD) patterns of compound SbOCl·DMSO show a strong correlation between the experimentally observed diffraction pattern and the theoretically calculated pattern based on single crystal X-ray diffraction data. This agreement confirms the purity of the experimental sample. In addition, to confirm the stability of the compound, we exposed the crystal to air for over 120 hours and performed powder XRD analysis on the sample after exposure. The results indicate that the sample does not undergo deliquescence and exhibits good stability.

The thermogravimetric analysis (TGA) curve of SbOCl·DMSO is shown in Fig. S1a.† It has been demonstrated that SbOCl·DMSO remains stable up to approximately 120 °C. PXRD analysis further confirms that Sb_2O_4 is the decomposition product of this compound (Fig. S1b†).

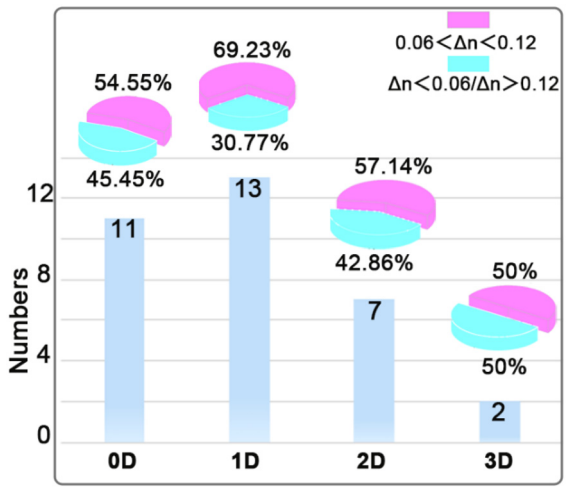

Fig. 4 Dimensional distribution statistics and birefringence distribution maps of the SbOCl·DMSO with the most Sb-based oxygen containing acid salt NLO crystals in each dimension. All data are available in Table S5 in the ESI.†

Optical properties

The UV-vis diffuse reflectance spectra of the SbOCl·DMSO compound are shown in Fig. 3b and c. The compound exhibits a bandgap of 3.74 eV, with a UV absorption edge around 331 nm, indicating that it possesses a wide transmission range and qualifies as an excellent NLO crystal.

The IR spectrum of SbOCl·DMSO is shown in Fig. S2.† The asymmetric stretching vibration of the Sb–O bond is observed at 607 cm^{-1}, while the bending vibration of the Sb–Cl bond appears at 501 cm^{-1}. The stretching vibration of the C–S bond is noted at 783 cm^{-1}. The peaks near 912/1350/3003 cm^{-1} can be attributed to the deformation vibration and asymmetric stretching vibration of CH_3 in DMSO. These vibrations are generally consistent with previously reported in the literature, confirming the presence of Sb–O/Cl and DMSO groups.[39,40]

The birefringence of SbOCl·DMSO was measured using a Zeiss Axio A5 polarizing microscope. As shown in Fig. 3d, the compound exhibits moderate birefringence of 0.084@546 nm. To better understand the relationship between structure and birefringence, we classified SbOCl·DMSO and other reported oxygen-containing Sb-based NLO crystals according to their structural dimensions, categorizing the birefringence ranges for compounds in each dimension (Fig. 4). The figure reveals that Sb-based oxygen-containing salts with a 1D structure dominate the distribution, with the highest proportion of compounds exhibiting moderate birefringence. This suggests that a 1D structure is more likely to result in moderate birefrin-

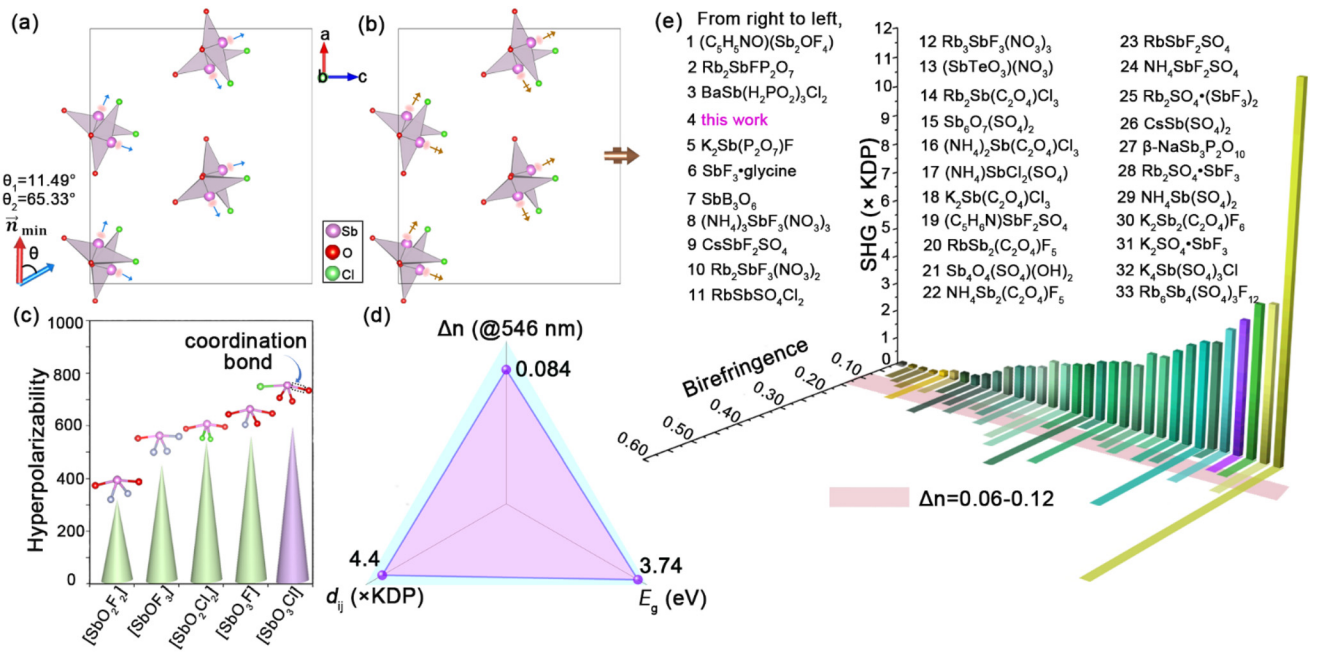

Fig. 5 (a) The angle diagram between the direction of lone pairs and the n_{min} in SbOCl·DMSO; (b) the orientation of dipole moments in the unit cell for $[SbO_3Cl]^{4-}$ groups in SbOCl·DMSO, the direction of the overall dipole moments is highlighted by brown arrow; (c) comparison the hyperpolarizability of $[SbO_2F_2]$, $[SbOF_3]$ $[SbO_2Cl_2]$, $[SbO_3F]$, and $[SbO_3Cl]$; (d) the radar plot of band gap E_g, SHG effect d_{ij} and Δn for SbOCl·DMSO; (e) the birefringence and SHG diagram for the SbOCl·DMSO with the most Sb-based oxygen-containing acid salt NLO crystals. All data are available in Table S5 in the ESI.†

gence. In the case of SbOCl·DMSO, the excellent 1D helical chain structure could play a crucial role in its moderate birefringence.

To further demonstrate the impact of functional groups on birefringence, we performed an in-depth analysis of the angle between the functional groups and the minimum optical axis (n_{min}). Pan *et al.* proposed that the smaller the angle between lone pair orientation and n_{min}, the greater the contribution of scalp metal cations to birefringence.[41] From the Fig. 5a, we can find that the angles between the SCALP electrons of Sb^{3+} and the direction of n_{min} not large (11.49°–65.33°), which helps the compound exhibit a large birefringence.

The SHG responses of SbOCl·DMSO were measured using the Kurtz–Perry method on sieved powder samples,[42] with a 1064 nm laser serving as the fundamental wave. As shown in Fig. 3e, the SHG effect of the compound gradually increased with increasing powder particles, indicating that the compound was type **I** phase-matchable. The compound endows a significant SHG effect of approximately 4.4 times that of KDP. In addition, we conducted a frequency doubling test on the sample after being placed in air for more than 120 hours (the purple line in Fig. 3e), and the test results showed that the signal of the compound did not change significantly, once again proving the stability of the compound. To provide a clearer explanation of the origin of the frequency doubling effect, the local dipole moments of $[SbO_3Cl]^{4-}$ seesaws were calculated (Table S4†). The results show that the polarizations in the x and y components are very small, while the z component exhibits a large value of 74.48 D for the superposition, which is consistent with the direction of the dipole moment of the $[SbO_3Cl]^{4-}$ triangular pyramid shown in Fig. 5b. In addition, we compared the hyperpolarizability of $[SbO_2F_2]$, $[SbOF_3]$ $[SbO_2Cl_2]$, $[SbO_3F]$, and $[SbO_3Cl]$ (Fig. 5c). Clearly, the introduction of Sb–O coordination bonds results in a significant increase in hyperpolarizability of $[SbO_3Cl]^{4-}$. These results indicate that the $[SbO_3Cl]^{4-}$ functional group makes significant contribution to the frequency doubling of the compound.

Excessive birefringence can hinder the practical application of NLO crystals by inducing drift effects and reducing conversion efficiency.[43] Therefore, it is crucial to synthesize NLO crystals with moderate birefringence, which balances optical performance and stability. In Fig. 5e, we compare the birefringence of the title compound with that of other Sb-based oxygen-containing acid salt NLO crystals.[24,25,31–33,44–66] Additionally, we

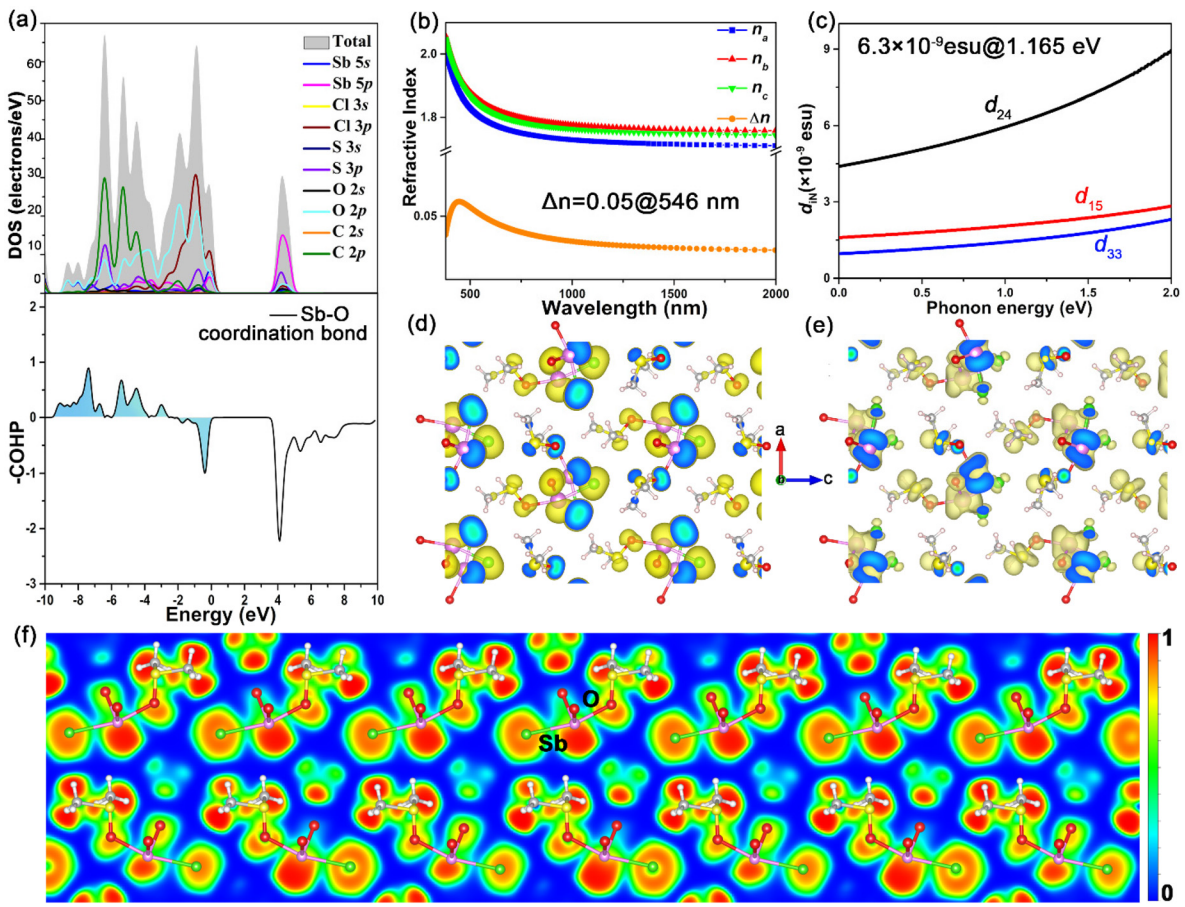

Fig. 6 (a) The total DOS, partial DOS and −COHP; (b) the calculated linear refractive indices; (c) the calculated frequency-dependent SHG coefficients for SbOCl·DMSO; the SHG density for (d) occupied and (e) unoccupied states in the VE process in SbOCl·DMSO; (f) the ELF map for SbOCl·DMSO.

compare their frequency doubling effects, as a large SHG coefficient directly enhances the conversion efficiency of NLO materials. It is evident that the reported compound exhibits a frequency doubling effect second only to $BaSb(H_2PO_2)_3Cl_2$ (5 × KDP, 0.09@546 nm), while maintaining moderate birefringence. The comparison results show that the compound is an excellent UV NLO crystal, which exhibits a good balance of large SHG coefficient (4.4 × KDP), moderate birefringence (0.084@546 nm) and short UV cut-off edge (331 nm) (Fig. 5d).

Theoretical calculation analysis

To further understand the relationship between the structure and optical properties of the compound SbOCl·DMSO, we carried out theoretical calculation using density functional theory (DFT) method.[67] The results show that the theoretical band gap of SbOCl·DMSO is 3.80 eV. It is basically in agreement with the experimental value of 3.74 eV, indicating that the calculation results are reasonable (Fig. S3†). The total and partial densities of states (TDOS and PDOS) are shown in Fig. 6a. The top of valence band (VB) is mainly contributed by the Cl 3p, O 2p, S 3p, C 2p and Sb 5p, and the bottom of conduction band (CB) is mainly contributed by the Sb 5p, S 3p and O 2p. It is well established that linear and nonlinear optical properties are predominantly influenced by the states near the Fermi level (E_f). Consequently, the synergistic effect of $[SbO_3Cl]^{4-}$ and [DMSO] contributes significantly to the outstanding optical properties of the compound. In addition, the –COHP analysis paired with PDOS highlights the bonding states between Sb and O that form coordination bonds near the E_f, further explaining their contribution to the optical properties of the material.

The refractive index dispersion curve of compound SbOCl·DMSO show that the compound is a biaxial crystal ($n_b > n_c > n_a$) (Fig. 6b). The theoretical calculation of the birefringence index is 0.05@546 nm, which closely aligns with our measured birefringence (0.084@546 nm). According to the space group and Kleinman symmetry, there exists three non-zero independent SHG tensor component. And the highest d_{24} is 6.3×10^{-9} esu@1.165 eV, which is closely with experimental value (Fig. 6c). Additionally, the SHG-weighted electron density of d_{24} for SbOCl·DMSO is investigated to dissect the origin of SHG response (Fig. 6d and e). Since the virtual electron (VE) processes of occupied and unoccupied states predominantly govern the SHG effects, it is evident that Sb atoms, O atoms, S atoms, and Cl atoms contribute to both occupied and unoccupied electronic states. This reaffirms that the $[SbO_3Cl]^{4-}$ and [DMSO] groups contributes significantly to the SHG response. In addition, the electron localization function (ELF) map was calculated (Fig. 6f), which exhibits the SCALP electrons on Sb atoms. And the coordination bonds between Sb and O atoms are proved.

Conclusions

In summary, we have successfully synthesized a novel NLO material, SbOCl·DMSO, which exhibits a perfect balance of optical properties: a short UV cut-off edge (331 nm), moderate birefringence (0.084@546 nm) and a large SHG coefficient (4.4 × KDP). The synergy between the $[SbO_3Cl]^{4-}$ and [DMSO] functional groups in the 1D helical chain structure is key to achieving these remarkable properties. This work paves the way for the design of high-performance NLO crystals incorporating SCALP electron systems and offers new insights into the future exploration of NLO materials.

Author contributions

The manuscript was written through contributions of all authors. Conceptualization, G. Z. and X. D.; methodology, X. P.; software, X. P., X. L. and Y. Z.; formal analysis, X. P. and L. H.; investigation, X. P.; resources, L. H., L. C. and D. G.; data curation, X. P.; writing – original preparation, X. P.; writing review & editing, G. Z. and X. D.; visualization, X. P. and X. L.; supervision, G. Z. and X. D.; project administration, G. Z. and X. D.; funding acquisition, X. D., L. H., L. C. and G. Z. All authors have given approval to the final version of the manuscript.

Data availability

The data supporting this article have been included as part of the ESI.†

Conflicts of interest

There are no conflicts to declare.

Acknowledgements

The authors thank Dr Daichuan Ma at the Analytical and Testing Center, Sichuan University for technical help in the Material Studio calculations. This work was supported by the National Natural Science Foundation of China (Grant No. 22305166, 22375139, 22201195), the Natural Science Foundation of Sichuan Province (2025ZNSFSC0910).

References

1 C. T. Chen, Y. B. Wang, B. C. Wu, K. C. Wu, W. L. Zeng and L. H. Yu, Design and Synthesis of an Ultraviolet-Transparent Nonlinear Optical Crystal $Sr_2Be_2B_2O_7$, *Nature*, 1995, **373**, 322–324.
2 D. F. Eaton, Nonlinear Optical Materials, *Science*, 1991, **253**, 281–287.
3 Y. Hou, H. P. Wu, H. W. Yu, Z. G. Hu, J. Y. Wang and Y. C. Wu, An Effective Strategy for Designing Nonlinear Optical Crystals by Combining the Structrure-Directing

Property of Oxyfluorides with Chemical Substitution, *Angew. Chem., Int. Ed.*, 2021, **60**, 25302–25306.
4 N. Savage, Ultraviolet Lasers, *Nat. Photonics*, 2007, **1**, 83–85.
5 Y. Chen, C. L. Hu, Z. Fang and J. G. Mao, $K_2Pb(H_2C_3N_3O_3)_4(H_2O)_4$: A Potential UV Nonlinear Optical Material with Large Birefringence, *Inorg. Chem. Front.*, 2021, **8**, 3547–3555.
6 Y. Q. Li, J. H. Luo and S. G. Zhao, Local Polarity-induced Assembly of Second-Order Nonlinear Optical Materials, *Acc. Chem. Res.*, 2022, **55**, 3460–3469.
7 H. X. Fan, N. Ye and M. Luo, New Functional Groups Design toward High Performance Ultraviolet Nonlinear Optical Materials, *Acc. Chem. Res.*, 2023, **56**, 3099–3109.
8 C. Wu, G. Yang, M. G. Humphrey and C. Zhang, Recent Advances in Ultraviolet and Deep-Ultraviolet Second-order Nonlinear Optical Crystals, *Coord. Chem. Rev.*, 2018, **375**, 459–488.
9 X. H. Dong, L. Huang and G. H. Zou, Rational Design and Controlled Synthesis of High-Performance Inorganic Short-Wave UV Nonlinear Optical Materials, *Acc. Chem. Res.*, 2025, **58**, 150–162.
10 T. L. Chao, W. J. Chang, S. H. Wen, Y. Q. Lin, B. C. Chang and K. H. Lii, Titanosilicates with Strong Phase-Matched Second Harmonic Generation Responses, *J. Am. Chem. Soc.*, 2016, **138**, 9061–9064.
11 Z. Y. Bai and K. M. Ok, Advances in Aliovalent Substitution Strategy for the Design and Synthesis of Nonlinear Optical Materials: d^0 Transition Metal/Gallium Iodates and Selenites, *Coord. Chem. Rev.*, 2023, **490**, 215212.
12 L. Kang and Z. S. Lin, Deep-Ultraviolet Nonlinear Optical Crystals: Concept Development and Materials Discovery, *Light: Sci. Appl.*, 2022, **11**, 201.
13 J. Chen, C. L. Hu, F. Kong and J. G. Mao, High-Performance Second-Harmonic-Generation (SHG) Materials: New Developments and New Strategies, *Acc. Chem. Res.*, 2021, **54**, 2775–2783.
14 G. H. Zou and K. M. Ok, Novel Ultraviolet (UV) Nonlinear Optical (NLO) Materials Discovered by Chemical Substitution-Oriented Design, *Chem. Sci.*, 2020, **11**, 5404–5409.
15 H. W. Yu, N. Z. Koocher, J. M. Rondinelli and P. S. Halasyamani, Pb_2BO_3I: A Borate Iodide with the Largest Second-Harmonic Generation (SHG) Response in the $KBe_2BO_3F_2$ (KBBF) Family of Nonlinear Optical (NLO) Materials, *Angew. Chem., Int. Ed.*, 2018, **57**, 6100–6103.
16 W. B. Zhang, X. L. Hou, S. J. Han and S. L. Pan, Toward the Ultraviolet (UV) or Deep-UV Nonlinear Optical Crystals: the Combination of π-Conjugated Planar $[XY_3]$ and Tetrahedral $[XY_4]$, *Coord. Chem. Rev.*, 2024, **505**, 215664.
17 F. Yang, L. J. Huang, X. Y. Zhao, L. Huang, D. J. Gao, J. Bi, X. Wang and G. H. Zou, An Energy Band Engineering Design to Enlarge the Band Gap of $KTiOPO_4$ (KTP)-type Sulfates via Aliovalent Substitution, *J. Mater. Chem. C*, 2019, **7**, 8131–8138.
18 W. Zeng, Y. Tian, H. M. Zeng, Z. E. Lin and G. H. Zou, Breaking Performance Barriers in $KBe_2BO_3F_2$(KBBF) Analogsby Functional Group Self-Polymerization, *Angew. Chem., Int. Ed.*, 2025, e202422818.
19 W. K. Wang, D. J. Mei, S. G. Wen, J. Wang and Y. D. Wu, Complex Coordinated Functional Groups: A Great Genes for Nonlinear Optical Materials, *Chin. Chem. Lett.*, 2022, **33**, 2301–2315.
20 F. Yang, L. Wang, L. Huang and G. H. Zou, The Study of Structure Evolvement of KTiOPO4 Family and Their Nonlinear Optical Properties, *Coord. Chem. Rev.*, 2020, **423**, 213491.
21 C. L. Hu, Q. Q. Chen, F. Kong and J. G. Mao, Discovery of Excellent Ultraviolet Nonlinear Optical Materials in Chlorates and Bromates with Highly Stereochemically Active Lone Pairs, *Inorg. Chem. Front.*, 2024, **11**, 3150–3158.
22 V. Nguyen, B. H. Ji, K. Wu, B. B. Zhang and J. Wang, Unprecedented Mid-Infrared Nonlinear Optical Materials Achieved by Crystal Structure Engineering, a Case Study of $(KX)P_2S_6$ (X = Sb, Bi, Ba), *Chem. Sci.*, 2022, **13**, 2640–2648.
23 J. Y. Guo, A. Tudi, S. J. Han, Z. H. Yang and S. L. Pan, Sn_2PO_4I: An Excellent Birefringent Material with Giant Optical Anisotropy in Non p-Conjugated Phosphate, *Angew. Chem., Int. Ed.*, 2021, **60**, 24901–24904.
24 L. Qi, X. X. Jiang, K. N. Duanmu, C. Wu, Z. S. Lin, Z. P. Huang, M. G. Humphrey and C. Zhang, Record Second-Harmonic Generation and Birefringence in an Ultraviolet Antimonate by Bond Engineering, *J. Am. Chem. Soc.*, 2024, **146**, 9975–9983.
25 B. Zhang, C. L. Hu, J. G. Mao and F. Kong, Fully Tricoordinated Assembly Unveils a Pioneering Nonlinear Optical Crystal $(SbTeO_3)(NO_3)$, *Chem. Sci.*, 2024, **15**, 18549–18556.
26 X. H. Dong, Y. Long, X. Y. Zhao, L. Huang, H. M. Zeng, Z. E. Lin, X. Wang and G. H. Zou, $A_6Sb_4F_{12}(SO_4)_3$ (A = Rb, Cs): Two Novel Antimony Fluoride Sulfates with Unique Crown-Like Clusters, *Inorg. Chem.*, 2020, **59**, 8345–8352.
27 G. J. Yi and G. H. Zou, Recent Advances on the Synthesis of Sb(III)-Based Inorganic Ultraviolet Nonlinear Optical Materials, *Chin. J. Struct. Chem.*, 2023, **42**, 100020.
28 L. Huang and G. H. Zou, Recent Progresses of UV Nonlinear Optical Materials, *Chin. J. Struct. Chem.*, 2020, **39**, 1571–1577.
29 P. Zhang, X. Mao, X. H. Dong, L. Huang, L. L. Cao, D. J. Gao and G. H. Zou, Two UV Organic-inorganic Hybrid Antimony-based Materials with Superior Optical Performance Derived from Cation-anion Synergetic Interactions, *Chin. Chem. Lett.*, 2024, **35**, 109235.
30 Y. Tian, W. Zeng, X. H. Dong, L. Huang, Y. Q. Zhou, H. M. Zeng, Z. E. Lin and G. H. Zou, Enhanced UV Nonlinear Optical Properties in Layered Germanous Phosphites through Functional Group Sequential Construction, *Angew. Chem., Int. Ed.*, 2024, **63**, e202409093.
31 X. H. Dong, H. B. Huang, L. Huang, Y. Q. Zhou, B. B. Zhang, H. M. Zeng, Z. E. Lin and G. H. Zou, Unearthing Superior Inorganic UV Second-Order Nonlinear Optical Materials: A Mineral-Inspired Method Integrating First-Principles High-Throughput Screening and Crystal Engineering, *Angew. Chem., Int. Ed.*, 2024, **63**, e202318976.

32 X. H. Dong, L. Huang, C. F. Hu, H. M. Zeng, Z. E. Lin, X. Wang, K. M. Ok and G. H. Zou, $CsSbF_2SO_4$: An Excellent Ultraviolet Nonlinear Optical Sulfate with a $KTiOPO_4$ (KTP)-type Structure, *Angew. Chem., Int. Ed.*, 2019, **58**, 6528–6534.

33 F. F. He, Y. L. Deng, X. Y. Zhao, L. Huang, D. J. Gao, J. Bi, X. Wang and G. H. Zou, $RbSbSO_4Cl_2$: An Excellent Sulfate Nonlinear Optical Material Generated Due to the Synergistic Effect of Three Asymmetric Chromophores, *J. Mater. Chem. C*, 2019, **7**, 5748–5754.

34 E. Alessio, Synthesis and Reactivity of Ru-, Os-, Rh-, and Ir-Halide–Sulfoxide Complexes, *Chem. Rev.*, 2004, **104**, 4203–4242.

35 Y. Lan, J. X. Ren, P. Zhang, X. H. Dong, L. Huang, L. L. Cao, D. J. Gao and G. H. Zou, $ASb(SO_4)_2$ (A = Rb, Cs): Two Short-wave UV Antimony Sulfates Exhibiting Large Birefringence, *Chin. Chem. Lett.*, 2024, **35**, 108652.

36 X. H. Dong, Z. Z. Zhang, L. Huang and G. H. Zou, $[C(NH_2)_3]BiCl_2SO_4$: An Excellent Birefringent Material Obtained by Multifunctional Group Synergy, *Inorg. Chem. Front.*, 2022, **9**, 5572–5578.

37 G. Q. Shi, Y. Wang, F. F. Zhang, B. B. Zhang, Z. H. Yang, X. L. Hou, S. L. Pan and K. R. Poeppelmeier, Finding the Next Deep-Ultraviolet Nonlinear Optical Material: $NH_4B_4O_6F$, *J. Am. Chem. Soc.*, 2017, **139**, 10645–10648.

38 K. Chen, Y. Yang, G. Peng, S. Yang, T. Yan, H. Fan, Z. Lin and N. Ye, $A_2Bi_2(SO_4)_2Cl_4$ (A = NH_4, K, Rb): Achieving a Subtle Balance of the Large Second Harmonic Generation Effect and Sufficient Birefringence in Sulfate Nonlinear Optical Materials, *J. Mater. Chem. C*, 2019, **32**, 9900–9907.

39 X. Y. Zhou, X. Mao, P. Zhang, X. H. Dong, L. Huang, L. L. Cao, D. J. Gao and G. H. Zou, Designing Excellent UV Birefringent Materials through the Synergistic Interaction of Two Highly Distorted Functional Groups, *Inorg. Chem. Front.*, 2024, **11**, 3221–3228.

40 O. V. Rudnitskaya, T. A. Tereshina, E. V. Dobrokhotova, E. K. Kultyshkina, I. A. Yakushev, N. A. Chumakova, A. I. Kokorin, Y. V. Zubavichus and V. N. Khrustalev, Chemical Evolution in Solutions of Ir Complex [H(dmso)$_2$]$_2$[$IrCl_6$]. Structures of [H(dmso)$_2$]$_2$[$IrCl_6$], [H(dmso)][$IrCl_4$(dmso)$_2$], [$Me_2SCH_2C(O)Me$][$IrCl_4$(dmso)$_2$], [$Me_2SCH_2C(O)Me$]$_2$[$IrCl_6$] and Its Os Analogue, *Eur. J. Inorg. Chem*, 2022, **33**, e202200463.

41 J. Y. Guo, A. Tudi, S. J. Han, Z. H. Yang and S. L. Pan, α-SnF_2: A UV Birefringent Material with Large Birefringence and Easy Crystal Growth, *Angew. Chem., Int. Ed.*, 2021, **60**, 3540–3544.

42 S. K. Kurtz and T. T. Perry, A powder technique for evaluation of nonlinear optical materials, *J. Appl. Phys.*, 1968, **39**, 3798–3813.

43 X. H. Dong, L. Huang, H. M. Zeng, Z. E. Lin, K. M. Ok and G. H. Zou, High-Performance Sulfate Optical Materials Exhibiting Giant Second Harmonic Generation and Large Birefringence, *Angew. Chem., Int. Ed.*, 2022, **61**, e202116790.

44 Y. Long, X. H. Dong, L. Huang, H. M. Zeng, Z. E. Lin, L. Zhou and G. H. Zou, $BaSb(H_2PO_2)_3Cl_2$: An Excellent UV Nonlinear Optical Hypophosphite Exhibiting Strong Second-harmonic Generation Response, *Mater. Today Phys.*, 2022, **28**, 100876.

45 S. V. Krivovichev and L. Bindi, Correspondence on "$K_2Sb(P_2O_7)F$: Cairo Pentagonal Layer with Bifunctional Genes Reveal Optical Performance", *Angew. Chem., Int. Ed.*, 2021, **60**, 3854–3855.

46 Z. Y. Bai, J. Lee, C. L. Hu, G. H. Zou and K. M. Ok, Hydrogen Bonding Bolstered Head-to-Tail Ligation of Functional Chromophores in a 0D SbF_3·glycine Adduct for a Short-Wave Ultraviolet Nonlinear Optical Material, *Chem. Sci.*, 2024, **15**, 6572–6576.

47 Y. C. Liu, X. M. Liu, S. Liu, Q. R. Ding, Y. Q. Li, L. N. Li, S. G. Zhao, Z. S. Lin, J. H. Luo and M. C. Hong, An Unprecedented Antimony(III) Borate with Strong Linear and Nonlinear Optical Responses, *Angew. Chem.*, 2020, **132**, 7867–7870.

48 Q. Wang, J. X. Ren, D. Wang, L. L. Cao, X. H. Dong, L. Huang, D. J. Gao and G. H. Zou, Low Temperature Molten Salt Synthesis of Noncentrosymmetric $(NH_4)_3SbF_3(NO_3)_3$ and Centrosymmetric $(NH_4)_3SbF_4(NO_3)_2$, *Inorg. Chem. Front.*, 2023, **10**, 2107–2114.

49 L. Wang, H. M. Wang, D. Zhang, D. J. Gao, J. Bi, L. Huang and G. H. Zou, Centrosymmetric $RbSnF_2NO_3$ vs. Noncentrosymmetric $Rb_2SbF_3(NO_3)_2$, *Inorg. Chem. Front.*, 2021, **8**, 3317–3324.

50 L. Wang, F. Yang, X. Y. Zhao, L. Huang, D. J. Gao, J. Bi, X. Wang and G. H. Zou, $Rb_3SbF_3(NO_3)_3$: an Excellent Antimony Nitrate Nonlinear Optical Material with a Strong Second Harmonic Generation Response Fabricated by a Rational Multi-component Design, *Dalton Trans.*, 2019, **48**, 15144–15150.

51 D. Zhang, Q. Wang, H. Luo, L. L. Cao, X. H. Dong, L. Huang, D. J. Gao and G. H. Zou, Deep Eutectic Solvents Synthesis of $A_2Sb(C_2O_4)Cl_3$ (A = NH_4, K, Rb) with Superior Optical Performance, *Adv. Opt. Mater.*, 2023, **11**, 2202874.

52 Q. Wei, C. He, K. Wang, X. F. Duan, X. T. An, J. H. Li and G. M. Wang, $Sb_6O_7(SO_4)_2$: A Promising Ultraviolet Nonlinear Optical Material with an Enhanced Second-harmonic-generation Response Activated by SbIII Lone-Pair Stereoactivity, *Chem. – Eur. J.*, 2021, **27**, 5880–5884.

53 F. F. He, Q. Wang, C. F. Hu, W. He, X. Y. Luo, L. Huang, D. J. Gao, J. Bi, X. Wang and G. H. Zou, Centrosymmetric $(NH_4)_2SbCl(SO_4)_2$ and Non-centrosymmetric $(NH_4)SbCl_2(SO_4)$: Synergistic Effect of Hydrogen-Bonding Interactions and Lone-Pair Cations on the Framework Structures and Macroscopic Centricities, *Cryst. Growth Des.*, 2018, **18**, 6239–6247.

54 W. Y. Wang, X. Y. Wang, L. Xu, D. Zhang, J. L. Xue, S. Y. Wang, X. H. Dong, L. L. Cao, L. Huang and G. H. Zou, Centrosymmetric $Rb_2Sb(C_2O_4)_{2.5}(H_2O)_3$ and Noncentrosymmetric $RbSb_2(C_2O_4)F_5$: Two Antimony(III) Oxalates as UV Optical Materials, *Inorg. Chem.*, 2023, **62**, 13148–13155.

55 Q. Wei, K. Wang, C. He, L. Wei, X. F. Li, S. Zhang, X. T. An, J. H. Li and G. M. Wang, Linear and Nonlinear Optical Properties of Centrosymmetric $Sb_4O_5SO_4$ and

Noncentrosymmetric $Sb_4O_4(SO_4)(OH)_2$ Induced by Lone Pair Stereoactivity, *Inorg. Chem.*, 2021, **60**, 11648–11654.

56 D. Zhang, Q. Wang, T. Zheng, L. Huang, L. L. Cao, D. J. Gao, J. Bi and G. H. Zou, $NH_4Sb_2(C_2O_4)F_5$: A Novel UV Nonlinear Optical Material Synthesized in Deep Eutectic Solvents, *J. Alloys Compd.*, 2022, **896**, 162921.

57 F. Yang, L. J. Huang, X. Y. Zhao, L. Huang, D. J. Gao, J. Bi, X. Wang and G. H. Zou, An Energy Band Engineering Design to Enlarge the Band Gap of $KTiOPO_4$ (KTP)-type Sulfates via Aliovalent Substitution, *J. Mater. Chem. C*, 2019, **7**, 8131–8138.

58 F. F. He, Y. W. Ge, X. Y. Zhao, J. He, L. Huang, D. J. Gao, J. Bi, X. Wang and G. H. Zou, Two-stage Evolution from Phosphate to Sulfate of New KTP-type Family Members as UV Nonlinear Optical Materials through Chemical Cosubstitutionoriented design, *Dalton Trans.*, 2020, **49**, 5276–5282.

59 Q. Wang, L. Wang, X. Y. Zhao, L. Huang, D. J. Gao, J. Bi, X. Wang and G. H. Zou, Centrosymmetric $K_2SO_4{\cdot}(SbF_3)_2$ and Noncentrosymmetric $Rb_2SO_4{\cdot}(SbF_3)_2$ Resulting from Cooperative Effects of Lone Pair and Cation Size, *Inorg. Chem. Front.*, 2019, **6**, 3125–3132.

60 Y. Lan, J. X. Ren, P. Zhang, X. H. Dong, L. Huang, L. L. Cao, D. J. Gao and G. H. Zou, $ASb(SO_4)_2$ (A = Rb, Cs): Two Short-wave UV Antimony Sulfates Exhibiting Large Birefringence, *Chin. Chem. Lett.*, 2024, **35**, 108652.

61 C. H. Hu, X. T. Cai, M. F. Wu, Z. H. Yang, J. Han and S. L. Pan, Lone Pair-driven Enhancement of Birefringence in Polar Alkali Metal Antimony Phosphates, *Chem. Mater.*, 2022, **34**, 4224–4231.

62 F. F. He, L. Wang, C. F. Hu, J. Zhou, Q. Li, L. Huang, D. J. Gao, J. Bi, X. Wang and G. H. Zou, Cation-tuned Synthesis of the $A_2SO_4{\cdot}SbF_3$ (A = Na^+, NH_4^+, K^+, Rb^+) Family with Nonlinear Optical Properties, *Dalton Trans.*, 2018, **47**, 17486.

63 Y. Lan, H. Luo, L. L. Wang, L. Huang, L. L. Cao, X. H. Dong and G. H. Zou, Two Short-wave UV Antimony(III) Sulfates Exhibiting Large Birefringence, *Inorg. Chem.*, 2024, **63**, 2814–2820.

64 D. Zhang, Q. Wang, T. Zheng, L. Cao, K. M. Ok, D. Gao, J. Bi, L. Huang and G. H. Zou, Cation-anion Synergetic Interactions Achieving Tunable Birefringence in Quasi-one-dimensional Antimony(III) Fluoride Oxalates, *Sci. China Mater.*, 2022, **65**, 3115–3124.

65 F. Yang, L. Wang, Y. W. Ge, L. Huang, D. J. Gao, J. Bi and G. H. Zou, $K_4Sb(SO_4)_3Cl$: The First Apatite-type Sulfate Ultraviolet Nonlinear Optical Material with Sharply Enlarged Birefringence, *J. Alloys Compd.*, 2020, **834**, 155154.

66 V. Y. Kavun, L. A. Zemnukhova and M. M. Polyantsev, Ion Mobility in Complex Antimony(III) Sulfate Fluorides $M_6Sb_4(SO_4)_3F_{12}$ (M = Rb, Cs, NH_4) and $(NH_4)_2Sb(SO_4)F_3$ According to ^{19}F and ^1H NMR Data, *J. Struct. Chem.*, 2018, **59**, 47–52.

67 S. I. Chu and D. A. Telnov, Beyond the Floquet Theorem: Generalized Floquet Formalisms and Quasienergy Methods for Atomic and Molecular Multiphoton Processes in Intense Laser fields, *Phys. Rep.*, 2004, **390**, 1–131.

